Inhibition of Nicotinic Acetylcholine Receptor by Philanthotoxin-343: Kinetic Investigations in the Microsecond Time Region Using a Laser-Pulse Photolysis Technique†

Vasanthi Jayaraman,‡,§ Peter N. R. Usherwood,‖ and George P. Hess*,‡

Section of Biochemistry, Molecular and Cell Biology, Division of Biological Sciences, 216 Biotechnology Building, Cornell University, Ithaca, New York 14853-2703, and Division of Molecular Toxicology, School of Biological Sciences, The University of Nottingham, Nottingham NG72RD, U.K.

Received May 27, 1999

ABSTRACT: The mechanism of inhibition of a nicotinic acetylcholine receptor (nAChR) in BC_3H1 muscle cells by philanthotoxin-343 (PhTX-343), a synthetic analogue of philanthotoxin-433, a wasp toxin, was investigated using a laser-pulse photolysis technique with microsecond time resolution and in a carbamoylcholine concentration range of 20−100 μM and PhTX-343 concentration range of 0−200 μM. The rate constant for nAChR channel opening determined by the chemical kinetic techniques decreased with increasing PhTX-343 concentration, whereas there was no significant effect on the rate constant for channel closing. The resulting decrease in the channel-opening equilibrium constant accounted quantitatively for the inhibition of the receptor by the toxin. Single-channel current measurements suggest an additional step in which the open channel:inhibitor complex isomerizes to a nonconducting receptor form. Cell-flow experiments with a time resolution of 10 ms indicate that this isomerization step is only important at very high inhibitor concentrations. The inhibitor binds to the open-channel receptor form, with an affinity that is at least 5 times smaller than that for the closed-channel form. This indicates that receptor inhibition mainly involves the binding of PhTX-343 to the closed-channel form of the receptor. PhTX-343, and an analogue of this polyamine, had no effect when applied to the inside of the cell membrane. However, there was significant inhibition of the nAChR when these compounds were applied to the outside of the cell membrane, indicating an extracellular site for inhibition. Furthermore, increasing the transmembrane potential results in a decrease in the ability of PhTX-343 to inhibit the receptor. This observation is related to the voltage dependence of the effect of PhTX-343 on the rate constant for nAChR channel opening with increasing transmembrane voltage (−60 to 50 mV). This suggests that the voltage dependence of inhibition mainly reflects the effect of transmembrane voltage on the rate constant of channel opening and, therefore, the channel-opening equilibrium constant. PhTX-343 competes with cocaine and procaine for its binding site. The finding that this toxin, which binds to a common inhibitory site with compounds such as cocaine, exerts its effect by decreasing the channel-opening equilibrium constant suggests an approach for the development of therapeutic agents. A compound that binds to this regulatory site but does not affect the channel-opening equilibrium constant may be developed. Such a compound can displace an abused drug such as cocaine and thereby alleviate the toxic effect of this compound on the organism.

Ionotropic neurotransmitter receptors are membrane-bound proteins that mediate transmission at synapses between neurons in the central nervous system and at neuromuscular junctions. Signal transmission between neurons involves the release of the neurotransmitter from one neuron that then binds to receptors on a second neuron. These receptors then form open transmembrane channels (*1*). The resulting flux of inorganic ions through such channels leads to a change in the transmembrane potential of the second neuron. Neurotransmitter receptors are inhibited by a wide variety of therapeutic compounds and abused drugs (*2*) and some natural toxins (*3*−*5*). Knowledge of the mechanisms (Figure 1) underlying such inhibition is essential for understanding the regulation of signal transmission in the nervous system and for the rational design of therapeutic agents targeted at ionotropic neurotransmitter receptors in the nervous system.

Philanthotoxin-343 (PhTX-343) (Figure 2A), a synthetic analogue of philanthotoxin-433, a wasp toxin, belongs to a class of polyamine amides that inhibits ionotropic neurotransmitter receptors, such as nicotinic acetylcholine (nAChR) and L-glutamate (GluR) receptors that form open cation-conducting channels (*3*, *4*). The mechanism of receptor

† This work was supported by a grant to G.P.H. from the National Institutes of Health (NS08527). V.J. was supported by a fellowship from the Cancer Research Fund of the Damon Runyon-Walter Winchell Foundation. P.N.R.U. was supported by a BIOME grant (BMH4-CT97-2395) from the European Commission.

* To whom correspondence should be addressed. Telephone: (607) 255-4809. Fax: (607) 255-2428. E-mail: gph2@cornell.edu.

‡ Cornell University.

§ Present address: Department of Chemistry, Marquette University, Milwaukee, WI 53201-1881.

‖ The University of Nottingham.

10.1021/bi991219x CCC: $18.00
Published on Web 08/14/1999

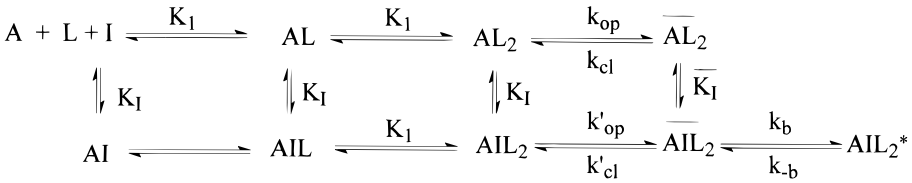

FIGURE 1: Minimum mechanism for the activation and inhibition of nAChR. A represents the receptor, L the neurotransmitter, and I the inhibitor. AI, AIL, and AIL_2 represent the complexes in which the inhibitor is bound to the closed-channel form of the receptor. $\overline{AIL_2}$ represents the inhibitor bound to the open-channel form of the receptor, and AIL_2* represents the nonconducting form of AIL_2. K_I and $\bar{K}_I$ are the observed dissociation constants for inhibitor binding to the closed- and open-channel forms, respectively; k_{op} and k_{cl} are the rate constants for channel opening and closing, respectively. k_b and k_{-b} are the rate constants for interconversion between the open channel (AIL_2) and the closed channel AIL_2*.

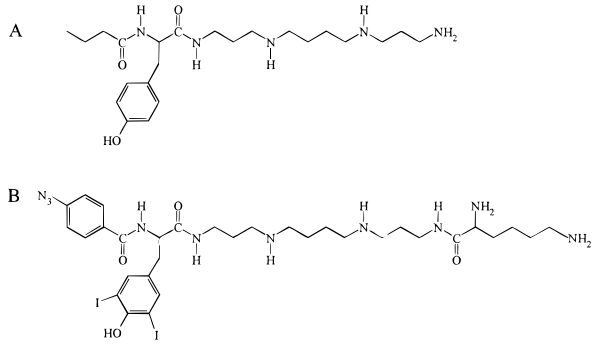

FIGURE 2: Structures of (A) PhTX-343 and (B) an analogue of PhTX-343 used by Choi et al. (*5*) for cross-linking experiments.

inhibition by PhTX-343 is of interest because of its possible therapeutic action as an inhibitor of the different receptors, in epilepsy or neurodegenerative diseases, or as a muscle relaxant (*6*). On the basis of electrophysiological measurements (*7*−*9*) and binding studies (*10*, *11*), a regulatory mechanism for the inhibition of nAChR and GluR by polyamine amides was proposed that involved the binding of toxin to the closed-channel forms of these receptors. However, under certain conditions, the toxins reduce the mean open times of nAChR (*10*) and GluR (*8*, *12*) channels, suggesting, in addition, an inhibitory site on the open-channel form (*8*, *10*, *12*). Recent cross-linking studies using a radiolabeled analogue of PhTX-343 with a photolabile group on one of its aromatic rings (Figure 2B) indicated that this PhTX-343 derivative preferentially cross-linked to a 20 kDa fragment of the α subunit of the nAChR (*5*). This 20 kDa fragment encompassed a large segment of the α subunit, containing the agonist-binding site and putative transmembrane segments M1−M3, as well as the α-bungarotoxin-binding site (*5*). However, since a 43 kDa protein that is associated with the receptor and present on the cytoplasmic side of the membrane (*5*) was also partially radiolabeled, it was suggested that PhTX-343 was bound to the α subunit on the intracellular side (*5*).

To differentiate between the various proposed mechanisms of inhibition, we determined the effects of inhibitors on the rate constants for channel opening and closing and on the dissociation constants for inhibition of the closed- and open-channel forms of the receptor. Recent development of a kinetic method with sub-millisecond time resolution that is suitable for chemical kinetic investigations of protein-mediated reactions on the surface of intact cells has made this differentiation between mechanisms possible (*13*−*17*). The technique involves equilibrating the cell with a photolabile inactive precursor of a compound that activates the receptor channel opening, photolyzing the compound to liberate the channel-activating ligand in the microsecond time region, and measuring the current which results from the opening of the receptor channels. Biologically inert photolabile compounds are now available that are photolyzed with half-time values between 15 and 45 μs. These compounds are suitable for transient kinetic investigations of nAChR (*13*) and GluR (*18*, *19*) and the ionotropic inhibitory receptors for γ-amino butyric acid (GABA) (*20*) and glycine (*21*). When this method was used to study the inhibition of the nAChR by procaine (*15*) and cocaine (*16*), the inhibition was found to involve predominantly a regulatory mechanism in which these noncompetitive inhibitors bound to both the closed- and open-channel forms of the receptor. This report describes fast kinetic studies of inhibition of the nAChR of BC_3H1 cells by PhTX-343 (Figure 2) (*22*).

MATERIALS AND METHODS

BC_3H1, a mammalian clonal cell line that expresses muscle-type nAChR (*23*), was cultured as described by Sine and Taylor (*24*). Carbamoylcholine was purchased from Sigma; caged carbamoylcholine synthesized according to the method of Milburn et al. (*13*) was a gift from Molecular Probes, and PhTX-343 and its analogue (*5*) were generous gifts from K. Nakanishi (Department of Chemistry, Columbia University, New York).

Cell-Flow and Laser-Pulse Photolysis. The flow device used for rapid solution exchange at the surface of a cell has been described in detail by Udgaonkar and Hess (*25*). A modified version of their device was used for measurements with cocaine and procaine, which allowed preincubation of the cell with cocaine and procaine before the application of carbamoylcholine (*15*, *16*). The observed current was corrected for receptor desensitization that occurs during equilibration of the cell surface receptors with the ligands in the flowing solution (*25*, *26*). The laser-pulse photolysis experiments were performed as described by Billington et al. (*27*). The photocleavage of the caged carbamoylcholine was initiated with a pulse of laser light generated by a Lumonics nitrogen excimer laser ($\lambda = 337$ nm). The output of the laser was coupled to an optical fiber (~200 μm in diameter), which delivered the light near the cell. The concentrations of caged carbamoylcholine were 200 and 750 μM, and the laser energies at the end of the fiber optic for the photolysis were ~250 and ~500 μJ, for the release of 20 and 100 μM carbamoylcholine, respectively.

For both the cell-flow and the laser-pulse photolysis experiments, the electrode solution contained 145 mM KCl, 10 mM NaCl, 2 mM $MgCl_2$, 1 mM EGTA, and 25 mM HEPES (pH 7.4); the extracellular bath solution contained

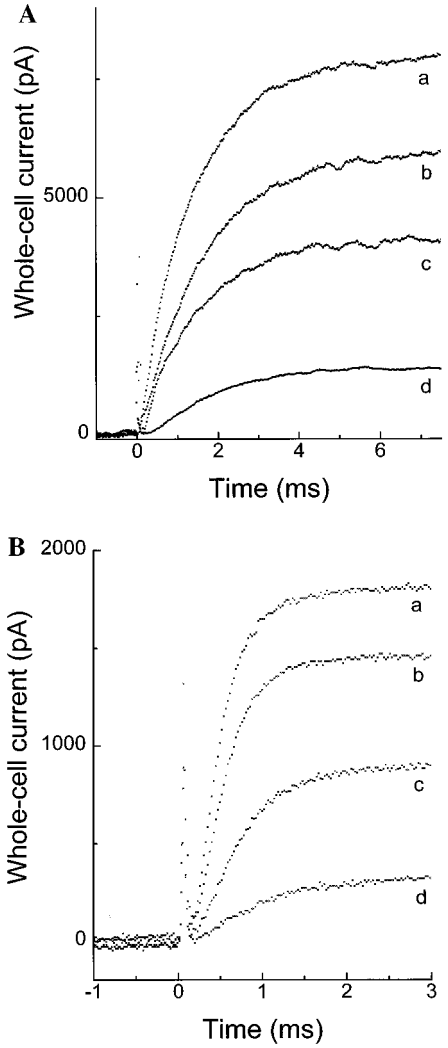

FIGURE 3: Whole-cell currents generated from laser-pulse photolysis of caged carbamoylcholine, with BC_3H1 cells at pH 7.4, 22 °C, and −60 mV. (A) Currents generated by release of 20 μM carbamoylcholine (a) in the absence and presence of (b) 25, (c) 50, and (d) 200 μM PhTX-343. The first-order rate constants of the whole-cell currents in traces a−d are 697 ± 4, 628 ± 5, 682 ± 7, and 625 ± 7 s^{-1}, respectively, and the maximum current amplitudes are 8119, 6119, 4170, and 1480 pA, respectively. (B) Currents generated by release of 100 μM carbamoylcholine (a) in the absence and presence of (b) 25, (c) 50, and (d) 200 μM PhTX-343. The first-order rate constants of the whole-cell currents in traces a−d are 2063 ± 25, 1666 ± 14, 1582 ± 17, and 1128 ± 24 s^{-1}, respectively, and the maximum current amplitudes are 1906, 1444, 878, and 359 pA, respectively.

140 mM NaCl, 5 mM KCl, 1.8 mM $CaCl_2$, 1.7 mM $MgCl_2$, and 25 mM HEPES (pH 7.4). Whole-cell currents recorded by the technique of Hamill et al. (*28*) were amplified with an Adams & List EPC-7 amplifier low-pass filtered at 1−5 kHz for the cell-flow experiments and at 20−30 kHz for the laser-pulse photolysis experiments. The filtered signal was digitized using a Labmaster DMA digitizing board controlled by Axon PClamp software at 0.5−1 kHz for the cell-flow and 20−35 kHz for the laser-pulse photolysis experiments. The data were analyzed using Origin 3.0 software.

Single-Channel Recording. The pipet solution used in these experiments contained carbamoylcholine with or without PhTX-343 in the extracellular buffer. The currents were recorded in a cell-attached mode (*28*, *29*).

Inside-out patches, in which the inside of the membrane faces the external solution, were obtained from the BC_3H1 cells as described by Sakmann and Neher (*29*). The electrode solution used in these experiments contained 1 μM carbamoylcholine in extracellular buffer. The inhibitor in the intracellular buffer was delivered to the inside of the membrane facing the outside using the same flow device that was used for the whole-cell recording measurements.

Outside-out patches were obtained from the cells as described by Sakmann and Neher (*29*). The electrode solution contained intracellular buffer. Carbamoylcholine (1 μM), with or without inhibitor in the extracellular buffer, was delivered from the same flow device that was used for the whole-cell recording measurements.

The currents for the above three measurements were amplified with an Adams & List EPC-7 amplifier and stored on magnetic tape. The data were low-pass filtered at 2 or 5 kHz using a Bessel filter (Dagan). The data were digitized and analyzed using Axon PClamp software and a Labmaster DMA digitizing board at the rate of 2 or 5 kHz. In the experiments with outside-out and inside-out membrane patches, the probability of an opening was obtained by determining the fraction of the time that the channel was open during a period of either 500 or 250 ms as indicated in the figure captions.

RESULTS AND DISCUSSION

Whole-cell currents obtained from BC_3H1 muscle cells upon photolysis of caged carbamoylcholine at various concentrations of PhTX-343 are shown in Figure 3. The whole-cell current decreases with increasing concentration of PhTX-343, at both 20 (Figure 3A) and 100 μM (Figure 3B) released carbamoylcholine.

Effect of PhTX-343 on Closed- and Open-Channel Conformations of the nAChR. A plot of the ratio of the maximum current obtained in the absence (I_0) and presence (I_I) of PhTX-343, at −60 mV, as a function of PhTX-343 concentration is shown in Figure 4 (solid lines), where the current is proportional to the concentration of the open receptor channels. The measurements are well represented by eq 1 (*30*):

$$\frac{I_0}{I_I} = 1 + \frac{[I]}{K_{I(obs)}} \quad (1)$$

where $K_{I(obs)}$ is the observed dissociation constant of the inhibitor.

It can been seen that the results obtained from cell-flow experiments (black symbols) and those obtained from laser-pulse photolysis experiments (white symbols) (Figure 4) agree within experimental error. This indicates that the corrected amplitude from the cell-flow measurements and those obtained directly in the laser-pulse photolysis experiments agree, as reported previously (*14*). This agreement between current amplitudes obtained by the two methods is also shown in Figure 4. It also indicates that neither the laser pulse nor the photolysis side products affect the kinetic measurements.

$K_{I(obs)}$ in eq 1 is the observed dissociation constant as given by eq 2:

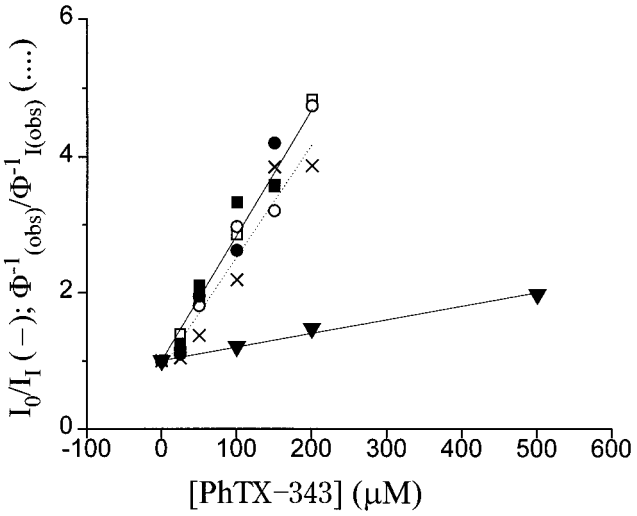

FIGURE 4: Ratio of the current amplitudes in the absence (I_0) and presence of PhTX-343 (I_I), obtained from cell-flow and laser-pulse photolysis measurements, with BC_3H1 cells at pH 7.4, 22 °C, and −60 mV, plotted as a function of PhTX-343 concentration (solid line). The maximum currents were obtained in the presence of 20 (■), 100 (●), and 750 μM carbamoylcholine (▲), and the white and black symbols represent the measurements obtained from laser-photolysis and cell-flow techniques, respectively. Each data point is the average of at least three measurements. The data are plotted according to eq 1 to evaluate the $K_{I(obs)}$ values. The value of $K_{I(obs)}$ obtained from the best fit (solid lines) with 20 and 100 μM carbamoylcholine is 53 ± 15 μM, and at 750 μM carbamoylcholine (solid line with the triangles) is 500 ± 240 μM. The calculated decrease in the current due to the decrease in the channel-opening equilibrium constant $\Phi^{-1}{}_I$ (×) is shown as the dotted line (eq 8).

$$\frac{I}{K_{I(obs)}} = \frac{FA}{K_{I1}} + \frac{FAL}{K_{I2}} + \frac{FAL_2}{K_{I3}} + \frac{\overline{FAL_2}}{K_{I4}} \qquad (2)$$

where FA, FAL, FAL_2, and $\overline{FAL_2}$ represent the fraction of receptors in the A, AL, AL_2, and $\overline{AL_2}$ forms, respectively. K_{I1}, K_{I2}, K_{I3}, and K_{I4} are the dissociation constants of PhTX-343 for dissociation from A, AL, AL_2, and $\overline{AL_2}$, respectively. Equation 2 can be approximated to

$$\frac{I}{K_{I(obs)}} = \frac{FA + FAL + FAL_2}{K'_I} + \frac{\overline{FAL_2}}{\bar{K}'_I} \qquad (3)$$

where K'_I and $\bar{K}'_I$ are the observed dissociation constants of the inhibitor from the closed- and open-channel forms of the nAChR, respectively. At low carbamoylcholine concentrations, when the receptor is predominantly in the closed form, $K_{I(obs)}$ reflects the dissociation constant of PhTX-343 for dissociation from the closed-channel forms of the receptor, and at high carbamoylcholine concentrations, it reflects the dissociation constant of PhTX-343 for dissociation from the open channel. The values of $K_{I(obs)}$ obtained from the slopes of the lines (Figure 4) are 53 ± 15 μM at both 20 μM carbamoylcholine and 100 μM carbamoylcholine and 500 ± 240 μM at 750 μM carbamoylcholine.

The dissociation constant for carbamoylcholine (K_1) and the channel-opening equilibrium constant for the activation of the acetylcholine receptor in BC_3H1 cells are 240 μM and 0.18, respectively (*25*). Using these values, the value of $FA + FAL + FAL_2$ changes by a factor of 1.4 between 20 and 100 μM and by a factor of ~4 between 20 and 750 μM carbamoylcholine. Since the inhibitor binds considerably better to the closed- than to the open-channel form (Figure 4) and the concentration of the closed-channel forms decreases by only a factor of 1.4 if the carbamoylcholine concentration is increased from 20 to 100 μM, it is not surprising that the values of $K_{I(obs)}$ do not change significantly in this concentration region (Figure 4 and eq 3).

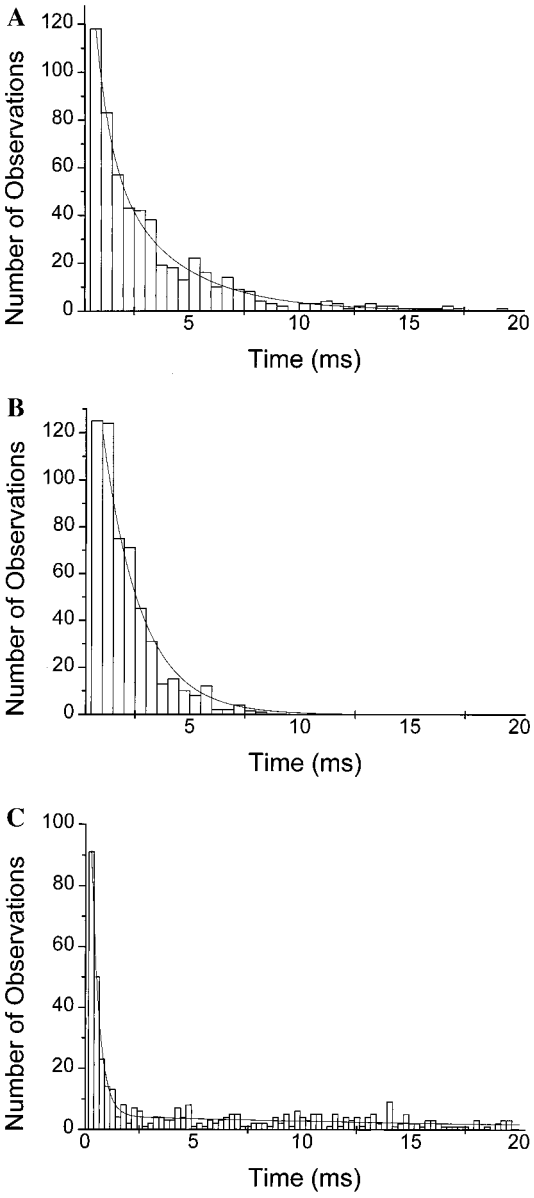

FIGURE 5: Histograms of the single-channel open and closed times, in BC_3H1 cells, at pH 7.4, −60 mV, and 22 °C, (a) in the presence of 1 μM carbamoylcholine represented by two exponentials with time constants of 0.8 ± 0.3 (35%) and 3.5 ± 0.1 ms (65%), and (b) in the presence of 1 μM carbamoylcholine and 25 μM PhTX-343 represented by one exponential with a time constant of 1.8 ± 0.1 ms. (c) Histogram of closed times in the presence of 1 μM carbamoylcholine and 25 μM PhTX-343 represented by two exponentials with time constants of 0.4 ± 0.1 and 12 ± 0.1 ms.

Inhibitory Site on the Open-Channel Form Observed with Single-Channel Measurements. Channel-opening events were also studied by single-channel measurements using 1 μM carbamoylcholine, in the presence and absence of PhTX-343 (Figure 5A−C). The number of openings decreased significantly upon increasing the PhTX-343 concentration. At 25 μM PhTX-343, channel openings had short closed

times (τ_b) (Figure 5C). The fast component in the closed time histogram had a time constant of 0.4 ms (Figure 5C); the second component with a time constant of 12 ms corresponds to the intermediate duration of closed times in the presence of low concentrations of carbamoylcholine first observed by Sine and Steinbach (*31*). In the presence of the inhibitor, the channels with a mean open time of 3.5 ms, observed in absence of the inhibitor, can no longer be detected. In the presence of 25 μM PhTX-343, the single-channel open times can be represented by a single-exponential distribution corresponding to a open channel lifetime of 1.8 ms (Figure 5B). Whether this distribution of open-channel lifetimes includes the lifetime of 0.8 ms seen in absence of toxin cannot be determined from our measurements. In previous experiments, the decrease in the mean open time of the nAChR channel in the presence of an inhibitor has been interpreted (*32*) to reflect the transition of the open receptor form $\bar{A}L_2$ (Figure 1) to a nonconducting receptor:inhibitor complex AIL_2* (Figure 1). Similarly, one of the brief closed times in experiments with PhTX-343 has a mean lifetime of 0.4 ms (Figure 5C). Such brief closed times have been interpreted to reflect the transition of the open channel blocked by inhibitor to the unblocked open channel (*32*). Our results are in agreement with these previous measurements (for instance, ref *32*) and their interpretations. The transient kinetic measurements that allow one to determine the rate constant for channel opening and the effect of inhibitors on this rate constant provide additional information. The transition of an open-channel inhibitor complex $\overline{AIL_2}$ to the closed-channel form AIL2 (Figure 1) is an example (Figure 1).

The commonly accepted inhibition process involves the binding of the inhibitor to the open channel and blocking it (Figure 1) (*32*−*38*). This mechanism requires that the time the channel spends in the open and blocked state in the presence of inhibitor should increase with increasing inhibitor concentration and that the current passing through the open channel remains the same in the presence and absence of inhibitor (*39*). This is not observed, under the conditions of the experiments whose results are shown in Figure 5. While the lifetime of the open channel in the absence of the toxin is 3.5 ms, the mean time interval the channel spends in the open and blocked state in the presence of inhibitor is 2.9 ms (data not shown). In addition, the current passing through the open channel decreases by a factor of 30% as the PhTX-343 concentration is increased to 25 μM (data not shown). The data are consistent with the mechanism based on the laser-pulse photolysis experiments in which $\overline{AIL_2}$ in Figure 1 can bypass the open-channel form $\overline{AL_2}$ and go directly to the closed-channel form AIL_2* (Figure 1). The consequences of this mechanism are that the resulting inhibitor-induced reduction of the channel-opening equilibrium constant can play a decisive role in receptor inhibition. It is important to point out that because the closed-channel form of the receptor binds PhTX-343 with an affinity at least 5 times higher than that of the open-channel form, the inhibition mechanism is dominated by the inhibitor binding to the closed-channel form, except at high concentrations of neurotransmitter (when the receptor is mainly in the open-channel form) and at very high concentrations of the toxin.

The transition from $\overline{AIL_2}$ to AIL_2* (Figure 1) can be observed at low carbamoylcholine concentrations in single-channel current measurements because one can observe the open channel directly. This equilibrium technique cannot be used at high carbamoylcholine concentrations because the receptor is rapidly converted to the inactive (desensitized) form.

Binding Site for PhTX-343 Probed Using Inside-Out and Outside-Out Membrane Patches. Cross-linking studies using a radiolabeled PhTX-343 analogue with a photolabile group (Figure 2B) suggested a possible intracellular site for binding (*5*). Inhibition of the nAChR by this analogue of PhTX-343 (Figure 2B) during its application to the extracellular and intracellular sides of the BC_3H1 cell membrane was probed using inside-out and outside-out membrane patches. Figure 6A−C shows the probability of a nAChR channel opening at −60 mV and at various times before and after application of the analogue of PhTX-343 (Figure 2B) on inside-out (Figure 6A) and outside-out membrane patches (Figure 6B). The probability of a channel opening decreases significantly upon applying 250 μM PhTX-343 analogue to outside-out patches within 250 ms of application of the toxin (Figure 6B). However, there is no significant change in the probability of a channel opening upon application of 250 μM PhTX-343 to inside-out patches for as long as 40 s (Figure 6A). This indicates that PhTX-343 and the PhTX-343 analogue (Figure 2B) inhibit by binding to an extracellular site of the nAChR.

Polyamines have been reported to inhibit nAChR when applied intracellularly at positive voltages (*40*). In oocytes, this inward rectification produces a decrease in the slope of the current−voltage relationship at positive voltages. However, in our studies, 250 μM PhTX-343 did not change the probability of channel opening when applied to inside-out patches at 60 mV (Figure 6D).

Effect of PhTX-343 on Channel-Opening and -Closing Rate Constants. The rising phase of the current in the laser-pulse photolysis experiments (Figure 3) follows a single-exponential rise for 85% of the reaction in all the measurements. The rise in the current reflects the formation of the open channels (*14*):

$$[\overline{AL_2}]_t = [\overline{AL_2}]_\infty(1 - e^{-k_{obs}t}) \quad (4)$$

$[\overline{AL_2}]$ represents the concentration of the receptors in the open-channel form and k_{obs} is the observed rate constant. The relationship between the observed rate constant and the rate constants for channel opening (k_{op}) and closing (k_{cl}), when the inhibitor binds to both the open- and closed-channel forms of the receptor, and the ligand-binding steps are fast compared to the channel-opening and -closing steps, is given by (*15*)

$$k_{obs} = k_{cl} + k_{op}\left(\frac{L}{L + K_1}\right)^2 \quad (5A)$$

in the absence of the inhibitor and by

$$k_{obs} = k_{cl}\left(\frac{\bar{K}_I}{\bar{K}_I + [I]}\right) + k_{op}\left(\frac{L}{L + K_1}\right)^2\left(\frac{K_I}{K_I + [I]}\right) \quad (5B)$$

in the presence of inhibitor, when L and $[I] \gg R_0$. L

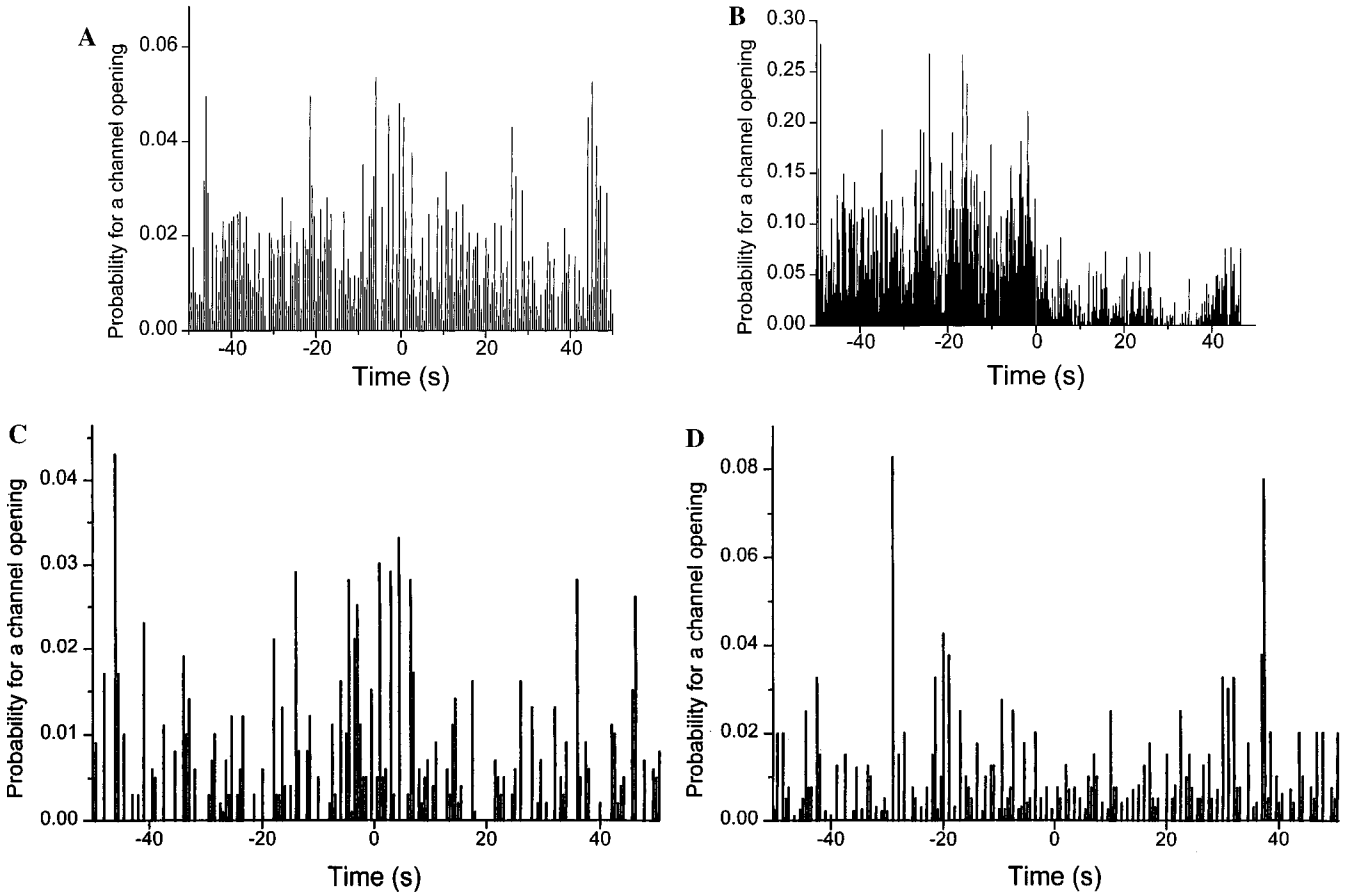

FIGURE 6: Probability of a channel opening at various times before (−50 to 0 s) and after (0 to 50 s) application of PhTX-343 or the PhTX-343 analogue, with (A) inside-out cell-membrane patches from BC_3H1 cells, using 1 μM carbamoylcholine and 250 μM PhTX-343 analogue, at −60 mV, averaged every 500 ms, (B) outside-out patches from BC_3H1 cells, using 1 μM carbamoylcholine and 250 μM PhTX-343 analogue, at −60 mV, averaged every 250 ms, (C) inside-out cell-membrane patches, using 1 μM carbamoylcholine and 250 μM PhTX-343, at −60 mV, averaged every 500 ms, and (D) inside-out patches, using 1 μM carbamoylcholine and 250 μM PhTX-343, at 60 mV, averaged every 500 ms. All the above experiments where performed at pH 7.4 and 22 °C.

represents the carbamoylcholine concentration, [I] the inhibitor concentration, and R_0 the concentration of receptor sites in the cell membrane. K_1 is the carbamoylcholine dissociation constant, and K_I and $\bar{K}_I$ are the dissociation constants for dissociation of the inhibitor from the open- and closed-channel forms of the receptor.

At low values of L, eq 5 reduces to

$$k_{obs} = k_{cl}\left(\frac{\bar{K}_I}{\bar{K}_I + [I]}\right) = k_{cl}' \qquad (6)$$

and at high values of L to

$$k_{obs} - k_{cl}' = \left[k_{op}\left(\frac{L}{L + K_1}\right)^2\right]\left[\frac{K_I}{[I] + K_I}\right] \qquad (7)$$

At 20 μM released carbamoylcholine, k_{obs} reflects k_{cl}' (eq 6), and as shown in Figure 7, there is no significant change in k_{cl} (□) in the concentration region of 0−200 μM PhTX-343. At 100 μM carbamoylcholine, $k_{obs} - k_{cl}$ (●) decreases by a factor of about 3 as the concentration of PhTX-343 is increased from 0 to 200 μM (Figure 7), implying a significant change in k_{op} (eq 7). The decrease in k_{op} implies a shift in the equilibrium toward the closed-channel form of the receptor upon increasing the PhTX-343 concentration. Since the maximum whole-cell current is determined by the fraction

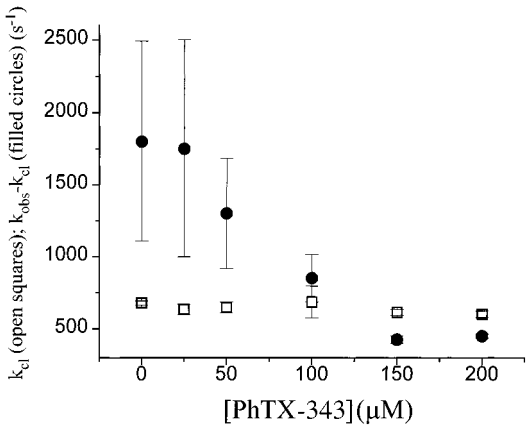

FIGURE 7: k_{cl} (□) and $k_{obs} - k_{cl}$ (●) plotted as a function of PhTX-343 concentration. Each data point is the average of at least three measurements. The observed first-order rate constants were measured from the rising phase of the whole-cell current generated by 20 μM released carbamoylcholine for k_{cl} and 100 μM released carbamoylcholine for $k_{obs} - k_{cl}$.

of receptors in the open-channel form (*25*), which in turn is determined by the channel-opening equilibrium constant ($\Phi^{-1} = k_{cl}/k_{op}$), a shift in the equilibrium constant toward the closed-channel form would result in the observed decrease in the current amplitude, seen in the experiments undertaken in the presence of PhTX-343. The experiment whose results are depicted in Figure 4 (dashed line) indicates

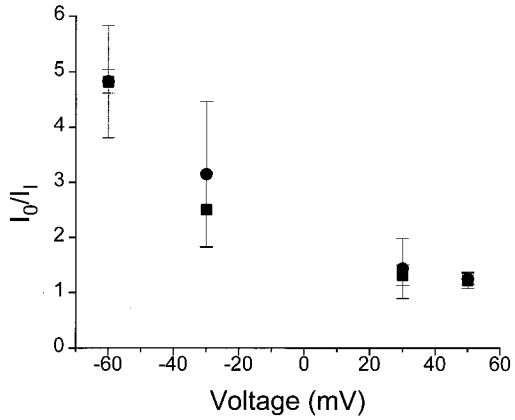

FIGURE 8: Ratio of the maximum current amplitudes in the absence (I_0) and presence of 200 μM PhTX-343 (I_I) obtained in the presence of 20 (■) and 100 μM (●) carbamoylcholine, plotted as a function of voltage. Each datum point is the average of at least three measurements.

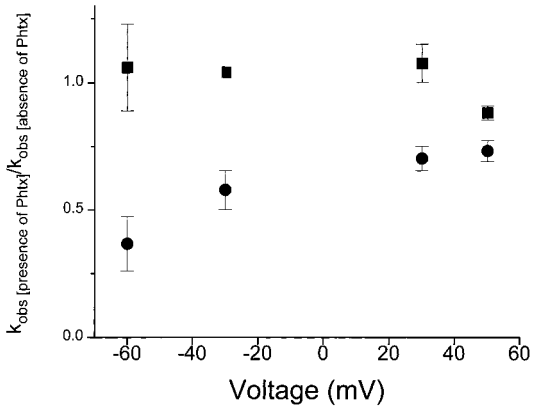

FIGURE 9: Ratio between k_{obs} in the presence of 200 μM PhTX-343 and k_{obs} in the absence of PhTX-343 obtained in the presence of 20 (■) and 100 μM (●) carbamoylcholine plotted as a function of voltage. Each data point is the average of at least three measurements.

that the extent of receptor inhibition, as determined by a decrease in the concentration of open receptor channels, is directly related to the change in the channel-opening equilibrium constant Φ^{-1} as a result of PhTX-343 binding to the receptor in the PhTX-343 concentration region of 0−200 μM, as shown in eq 8.

$$\frac{\Phi^{-1}_{(obs)}}{\Phi^{-1}_{I(obs)}} = \left(\frac{k_{op}}{k_{CL}}\right)\left[\frac{k_{op}\left[\frac{k_{I(obs)}}{k_{I(obs)} + [I]}\right]}{k_{CL}}\right]^{-1} = 1 + \frac{[I]}{K_{I(obs)}} \quad (8)$$

where $\Phi^{-1}_{(obs)}$ and $\Phi^{-1}_{I(obs)}$ are the observed channel-opening equilibrium constants in the absence and presence of inhibitor, respectively. $K_{I(obs)}$ represents the observed dissociation constant for dissociation from the closed-channel form, and the value of k_{cl} is not affected by the toxin (Figure 7). It should be noted from the results depicted in Figure 7 that at a PhTX-343 concentration of 200 μM the k_{obs} value for channel opening (eq 5B) is dominated by k_{cl}.

The plot of $\Phi^{-1}_{(obs)}/\Phi^{-1}_{I(obs)}$ according to eq 8 is shown in Figure 4 (crosses, dotted line). As can be seen, the decrease in the ratio of $\Phi^{-1}_{(obs)}/\Phi^{-1}_{I(obs)}$ in the presence of PhTX-343 due to the decrease in the channel-opening equilibrium constant (eq 8) is the same as that of the ratio of the maximum currents, I_0/I_I, determined in the whole-cell current measurements in cell-flow (■) and laser-pulse photolysis experiments (□) (Figure 4). The calculated K_I from the slope of the dashed line, calculated from the ratio of the channel-opening equilibrium constant in the presence and absence of inhibitor, is 60 ± 10 μM, which is in good agreement with that obtained from the cell-flow and laser-pulse photolysis experiments in which the whole-cell current is measured and in which the observed K_I is 53 ± 15 μM. These results indicate that at low concentrations of carbamoylcholine, the PhTX-343-induced decrease in k_{op}' without a concomitant change in k_{cl}' accounts for the decrease in the extent of channel opening in the channel-opening equilibrium constant and for the inhibition due to PhTX-343 at low carbamoylcholine concentrations when the receptor is mainly in the closed-channel form.

Voltage Dependence of Inhibition by PhTX-343. The relationship between the membrane voltage and the ratio of the maximum current in the absence (I_0) and presence (I_I) of 200 μM PhTX-343 is shown in Figure 8. The maximum currents were obtained from photolysis experiments in which 20 (■) and 100 μM (●) carbamoylcholine were released. These graphs indicate that the inhibition by PhTX-343 is voltage-dependent and the extent of inhibition decreases upon increasing the membrane potential.

In Figure 9, the ratio of the k_{obs} for the rise of the current elicited by 20 (squares) and 100 μM (circles) carbamoylcholine in the presence of 200 μM PhTX-343 to the k_{obs} in the absence of PhTX-343 is plotted as a function of voltage. There is no significant change in this quantity with 20 μM carbamoylcholine, but an increase is observed with 100 μM carbamoylcholine at positive voltages. Since at 20 μM carbamoylcholine k_{obs} reflects k_{cl}, whereas at 100 μM it reflects both k_{cl} and k_{op} (eq 7), it can be concluded that k_{cl} does not change as a function of voltage, but that k_{op}' in the presence of the toxin decreases by about a factor of 3 at 60 mV compared to the value at −60 mV. Hence, the observed voltage-dependent change of the extent of inhibition by PhTX-343 can be attributed in part to the effect of voltage on the effect of PhTX-343 on the k_{op}'.

Inhibition by PhTX-343 in the Presence of Cocaine and Procaine. The kinetic results described above indicate that PhTX-343 inhibits predominantly by binding to the closed-channel form of the nAChR. A similar study of cocaine inhibition indicated a similar mechanism (*16*). To determine if these inhibitors compete for the same binding site on the closed-channel form of nAChR or if they are binding to two different sites, the inhibition was studied in the presence of PhTX-343 and cocaine and of PhTX-343 and procaine.

When two inhibitors I′ and I″ with observed dissociation constants K' and K'', respectively, bind to the same inhibitory site, a receptor can have only one or the other inhibitor bound (AI′ or AI″, ALI′ or ALI″, etc.). Hence, the ratio of the maximum current (I_0/I_I) in the presence of the two inhibitors I′ and I″, respectively, is given by

$$\frac{I_0}{I_I} = 1 + \frac{[I']}{K'_{I(app)}} + \frac{[I'']}{K''_{I(app)}} \quad (9)$$

When the concentration of inhibitor I′ is kept constant and that of inhibitor I″ is varied, the slope of the line will be the

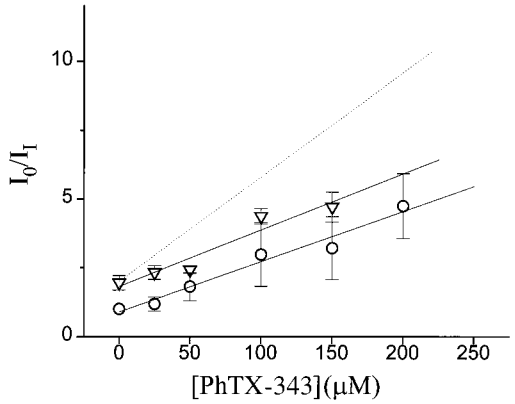

FIGURE 10: Ratio of the current amplitudes in the absence (I_0) and presence (I_I) of PhTX-343 obtained from cell-flow experiments with BC_3H1 cells at pH 7.4, 22 °C, and −60 mV plotted as a function of PhTX-343 concentration in the presence of 100 μM cocaine (▽) and in the absence of cocaine (○). The maximum currents were obtained in the presence of 20 μM carbamoylcholine and after preincubation for 4 s with cocaine and PhTX-343. The dashed line represents the hypothetical case in which PhTX-343 and cocaine bind to a different site (eq 10). The value of the intercept $[1 + [I']/K'_{I(app)}]$ from the plot (▽), which is 1.8, was used in conjunction with eq 10 to obtain the theoretical line.

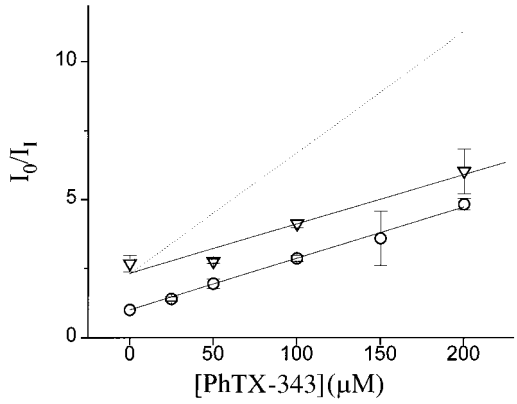

FIGURE 11: Ratio of the current amplitudes in the absence (I_0) and presence of PhTX-343 (I_I) obtained from cell flow with BC_3H1 cells at pH 7.4, 22 °C, and −60 mV, plotted as a function of PhTX-343 concentration, in the absence (○) and in the presence of 75 μM procaine (▽). The maximum currents were obtained in the presence of 20 μM, and after preincubation for 4 s with cocaine and PhTX-343. The dashed line represents the hypothetical case in which PhTX-343 and procaine bind to a different site (eq 10). The value of the intercept $[1 + [I']/K'_{I(app)}]$ from the plot (▽), which is 2.3, was applied to eq 10 to obtain the theoretical line.

same as that obtained in the absence of inhibitor I′ but the intercept will change. However, for inhibitors that bind to two different sites, in addition to receptors with one inhibitor bound there may also be receptors with both inhibitors bound (AI′I″, ALI′I″, etc.). Hence, the ratio of the maximum current in the presence of the two inhibitors (I_I) to that in their absence (I_0) would be

$$\frac{I_0}{I_I} = 1 + \frac{[I']}{K'_{I(app)}} + \frac{[I'']}{K''_{I(app)}}\left[1 + \frac{[I']}{K'_{I(app)}}\right] \qquad (10)$$

When the concentration of inhibitor I′ is kept constant and that of inhibitor I″ is varied, both the slope of the line and the intercept will be different than in an experiment in which I′ is absent. In Figure 10, the ratio of the maximum current obtained with 20 μM carbamoylcholine at various concentrations of PhTX-343 and in the presence of 100 μM cocaine (△) is compared to that obtained in the absence of cocaine (○). The slope of the lines in Figure 10 is the same in the presence or absence of 100 μM cocaine, implying that PhTX-343 competes with cocaine (eq 9). The dashed line in Figure 10 indicates what would be expected if cocaine and PhTX-343 bind to different sites; the slope is much steeper than in the case where the two inhibitors bind to the same site. Similar measurements at various concentrations of PhTX-343 in the presence of 75 μM procaine are shown in Figure 11. The slope for the extent of inhibition by PhTX-343 in the presence of procaine is the same as that in its absence, indicating that PhTX-343 and procaine compete for the same site on the closed-channel form of nAChR.

CONCLUSION

The chemical kinetic measurements indicate that the affinity of PhTX-343 is ∼5-fold greater for the closed-channel form of the nAChR than for the open-channel form. This implies that PhTX-343 inhibits predominantly by binding to the closed-channel form.

The observed rate constant for channel opening determined by the laser-pulse measurements at low carbamoylcholine concentrations at which it reflects k_{cl} (eq 5A) does not change significantly with increasing PhTX-343, but does decrease significantly at higher carbamoylcholine concentrations at which it reflects k_{op} (eq 5B) (Figure 7). The experiments indicate, therefore, that there is no significant change in the observed rate constant for channel closing when the PhTX-343 concentration is increased. The decrease in the observed rate constant for channel opening at high concentrations of carbamoylcholine implies that the rate constant for channel opening decreases with increasing PhTX-343 concentrations. Thus, increasing concentrations of PhTX-343 shift the channel-opening equilibrium toward the closed-channel state (Figure 1), which is observed as a decrease in current in the presence of PhTX-343 (Figure 4). The shift in the channel-opening equilibrium due to the decrease in k_{op} in the presence of PhTX-343 accounts quantitatively for the inhibition by PhTX-343 at low carbamoylcholine concentrations (Figure 4).

The single-channel current measurements (Figure 5) indicate an inhibitory site on the open-channel form of nAChR. The dissociation constant of the inhibitory site from the open form is ∼500 μM as observed by cell-flow measurements at 750 μM carbamoylcholine (Figures 5) and is considerably higher than that of the closed-channel form value of ∼50 μM.

Inhibition of the nAChR by PhTX-343 and its analogue (Figure 2) was observed only when the compounds were applied to outside-out patches. PhTX-343 and its analogue had no effect when they were applied to inside-out patches (Figure 6), indicating that the binding site for polyamines is on the extracellular side of the nAChR of BC_3H1 cells.

The extent of inhibition of the nAChR by PhTX-343 is voltage-dependent and decreases at more positive voltages. This can be attributed to a large extent to a decreasing effect of PhTX-343 on k_{op}' and, therefore, on the channel-opening equilibrium constant (see eq 8) as the voltage is increased from −60 to 50 mV (Figure 9). Thus, the voltage dependence of the inhibition cannot be used as an indicator for an inhibitory site on the open-channel form (*33*).

The $K_{I(obs)}$ value of PhTX-343 is unaffected by the presence of cocaine or procaine (Figures 10 and 11). This indicates that these inhibitors do not act independently but that they bind to the same or overlapping inhibitory sites of the nAChR.

On the basis of the observations described here, it can be concluded that PhTX-343 acts predominantly by a regulatory mechanism in which it binds to a regulatory site of the closed-channel form of the nAChR and, thereby, allosterically inhibits signal transmission by decreasing the channel-opening equilibrium constant. Under physiological conditions, where the concentrations of neurotransmitter and toxin are low, receptor inhibition is explained by this mechanism. At very high concentrations of neurotransmitter and inhibitor, an additional inhibitory process is observed in which the complex of the inhibitor with the open-channel form isomerizes to a nonconducting receptor form.

The finding reported here that an inhibitor binding to a regulatory site of the receptor changes the channel-opening equilibrium constant opens up the possibility for the development of therapeutic agents that would also compete for this binding site, without affecting the channel-opening equilibrium constant. Such a compound can bind to this site by displacing an abused drug such as cocaine and, thereby, alleviate the toxic effect of such compounds on the organism.

REFERENCES

1. Kandel, E. R., Schwartz, J. H., and Jessel, T. M. (1995) *Essentials of Neural Science and Behaviour*, Appleton & Lange, Norwalk, CT.
2. Gilman, A. G., Rall, T. W., Nies, A. S., and Taylor, P. (1990) *Goodman and Gilman's The Pharmacological Basis of Therapeutics*, Pergamon Press, New York.
3. Usherwood, P. N. R., and Blagbrough, I. S. (1992) *Pharmacol. Ther. 52*, 245−268.
4. Usherwood, P. N. R (1994) *Advances in Insect Physiology*, Vol. 24, pp 361, Academic Press, London.
5. Choi, S.-K., Kalivretenos, A. G., Usherwood, P. N. R., and Nakanishi, K. (1995) *Chem. Biol. 2*, 23−32.
6. Chapman, A. G. (1996) in *Excitatory Amino Acid Antagonists* (Meldrum, B. S., Ed.) Blackwell Scientific Publications, Boston.
7. Brackley, P. T. H., Bell, D. R., Choi, S.-K., Nakanishi, K., and Usherwood, P. N. R. (1993) *J. Pharmacol. Exp. Ther. 266*, 1573−1580.
8. Kerry, C. J., Ramsey, R. L., Sansom, M. S. P., and Usherwood, P. N. R. (1998) *Brain Res. 459*, 312−323.
9. Donovan, S. D., and Rogawski, M. (1996) *Neuroscience 70*, 361−375.
10. Rozental, R., Scoble, G. T., Albuquerque, E. X., Idriss, M., Sherby, S., Sattelle, D. B., Nakanishi, K., Konno, K., Eldefrawi, A. T., and Eldefrawi, M. E. (1989) *J. Pharmacol. Exp. Ther. 249*, 123−130.
11. Anis, N., Sherby, S., Goodnow, R., Jr., Niwa, M., Konno, K., Kallimopoulos, T., Bukownik, R., Nakanishi, K., Usherwood, P., Eldefrawi, A. T., and Eldefrawi, M. E. (1990) *J. Pharmacol. Exp. Ther. 254*, 765−773.
12. Antonov, S. M., Dudel, J., Franke, C., and Hatt, H. (1989) *J. Physiol. 419*, 569−588.
13. Milburn, T., Matsubara, N., Billington, A. P., Udgaonkar, J. B., Walker, J. W., Carpenter, B. K., Webb, W. W., Marque, J., Denk, W., McCray, J. A., and Hess, G. P. (1989) *Biochemistry 29*, 49−55.
14. Matsubara, N., Billington, A. P., and Hess, G. P. (1992) *Biochemistry 31*, 5507−5514.
15. Niu, L., and Hess, G. P. (1993) *Biochemistry 32*, 3831−3835.
16. Niu, L., Abood, L. G., and Hess, G. P. (1995) *Proc. Natl. Acad. Sci. U.S.A. 92*, 12008−12012.
17. Hess, G. P., and Grewer, C. (1998) *Methods Enzymol. 291*, 443−473.
18. Wieboldt, R., Gee, K. R., Niu, L., Ramesh, D., Carpenter, B. K., and Hess, G. P. (1994) *Proc. Natl. Acad. Sci. U.S.A. 91*, 8752−8756.
19. Niu, L., Gee, K. R., Schaper, K., and Hess, G. P. (1996) *Biochemistry 35*, 2030−2036.
20. Gee, K. R., Wieboldt, R., and Hess, G. P. (1994) *J. Am. Chem. Soc. 116*, 8366−8367.
21. Niu, L., Wieboldt, R., Ramesh, D., Carpenter, R. K., and Hess, G. P. (1996) *Biochemistry 35*, 8136−8142.
22. Eldefrawi, A. T., Eldefrawi, M. E., Konno, K., Mansour, N. A., Nakanishi, K., Oltz, E., and Usherwood, P. N. R. (1988) *Proc. Natl. Acad. Sci. U.S.A. 85*, 4910−4913.
23. Schubert, D., Harris, A. J., Devine, E. E., and Heinemann, S. (1974) *J. Cell Biol. 61*, 398−402.
24. Sine, S. M., and Taylor, P. (1979) *J. Biol. Chem. 254*, 3315−3325.
25. Udgaonkar, J. B., and Hess, G. P. (1987) *Proc. Natl. Acad. Sci. U.S.A. 84*, 8758−8762.
26. Hess, G. P., Udgaonkar, J. B., and Olbricht, W. L. (1987) *Annu. Rev. Biophys. Chem. 16*, 507−534.
27. Billington, A. P., Matsubara, N., Webb, W. W., and Hess, G. P. (1992) *Tech. Protein Chem. 3*, 417−427.
28. Hamill, O. P., Marty, A., Neher, E., Sakmann, B., and Sigworth, F. J. (1981) *Pfluegers Arch. 391*, 85−100.
29. Sakmann, B., and Neher, E., Eds. (1995) *Single-channel Recording*, Plenum, New York.
30. Karpen, J. W., and Hess, G. P. (1986) *Biochemistry 25*, 1777−1785.
31. Sine, S. M., and Steinbach, J. H. (1986) *J. Physiol. 373*, 124−162.
32. Neher, E., and Steinbach, J. H. (1978) *J. Physiol. 277*, 153−176.
33. Adams, P. R. (1976) *Pfluegers Arch. 361*, 145−151.
34. Ogden, D. C., and Colquhoun, D. (1985) *Proc. R. Soc. London, Ser. B 225*, 329−355.
35. Karlin, A. (1991) *Harvey Lect. 85*, 71−107.
36. Galzi, J. L., Revah, F., Bessis, A., and Changeux, J. P. (1991) *Annu. Rev. Pharmacol. 31*, 37−72.
37. Lester, H. A. (1992) *Annu. Rev. Biophys. Biomol. Struct. 21*, 267−292.
38. Lena, C., and Changeux, J. P. (1993) *Trends Neurosci. 16*, 181−186.
39. Neher, E. (1983) *J. Physiol. 339*, 663−678.
40. Haghighi, A., and Cooper, E. (1997) *Biophys. J. 72*, A264.

BI991219X